Dynamical control of systems near bifurcation points using time series

Zhao Hong,[1,2,*] Liu Yaowen,[2] Ping Huican,[2] and Wang Yinghai[2]
[1]*CCAST (World Laboratory), P.O. Box 8730, Beijing 100080, China*
[2]*Department of Physics, Lanzhou University, Lanzhou 730000, China*[†]

(Received 19 January 1999; revised manuscript received 4 June 1999)

In order to excite experimentalists to apply a dynamical control method [Zhao *et al.*, Phys. Rev. E **53**, 299 (1996); **57**, 5358 (1998)], we further introduce a simplified control law in this paper. The law provides a convenient way (in certain circumstance a necessary way) for experimentalists to achieve the system control when the exact position of the desired control objective cannot be known in advance. The validity of the control law is rigidly verified when the system nears a bifurcation point but our numerical examples show that it can be extended to a wide parameter region practically.

PACS number(s): 05.45.−a

I. INTRODUCTION

Dynamical control of experimental systems has drawn great research interests due to its potential applications in various fields. A lot of control methods have been presented in the past decade and many of them have been proven to be useful in experiments. The purpose of this paper is to introduce a new control law to experimentalists. For simplicity of the discussion, we consider a simple one-dimensional map

$$x_{i+1}=f(x_i,p) \tag{1}$$

in this section, where $x\in R$ and p is an adjustable parameter. To stabilize a fixed point x_* (we only discuss the case of fixed point in this paper when explaining the principle; the extension for period orbit is direct) of the system, one can add perturbations to the parameter p. According to the form of the perturbation laws, we can classify the present control methods into two classes. The first class is based on the perturbation law

$$p_{i+1}=p_0+k(x_{i+1}-x_*). \tag{2}$$

This form is indeed a very basic one used in the control theory (see, for example, Ref. [1]). Ott, Grebogi, and Yorke presented a technique of calculating specific value of the coefficient k employing the knowledge of the local stability of the fixed point in 1990 [2]. Thereafter chaos control has been considered an intensive topic. The control law in the form of Eq. (2) can be called the ''prompt linear feedback law'' since the prompt measured information x_{i+1} is used to construct the linear feedbacks. This control law is adopted in most of the articles concerning chaos control [3–5].

As the second class, we refer to the control methods using perturbation forms different from the prompt linear feedback law. In this direction, Pyragas presented [6] a feedback law whose discrete version can be written as

$$p_{i+1}=p_0+k(x_{i+1}-x_i). \tag{3}$$

The most important feature of Eq. (3) is that the desired objective x_* is replaced by the delayed record x_i. This feature makes the law (3) suitable for the control of dynamical systems without knowing the desired objectives in advance, therefore enlarges the scope of dynamical system controls. This law has also been applied to many experimental situations [7]. However, its validity has not been proven theoretically. Does the solution guaranteeing the stability of systems always exist? The answer is negative as will be clear at the end of this section. Some of the present authors have proposed [8,9] a general mathematical framework for different forms of feedback laws, with emphasis on two specific control laws belonging to the second class. One is

$$p_{i+1}=p_0+k(x_i-x_*)+k'(p_i-p_0) \tag{4}$$

and the other is

$$p_{i+1}=p_0+k(x_{i+1}-x_i)+k'(p_i-p_0). \tag{5}$$

The former can stabilize x_* using the previous state x_i when the prompt information of x_{i+1} is not accessible in time. While the latter has three functions: (a) stabilizing the unstable orbit, (b) tracking the desired orbit when the system parameters change as a function of time, and (c) targeting the unstable orbit from the stable one created at the same tangential bifurcation point without knowing the position of the unstable one in advance.

In the present paper we do not want to repeat the law (4). What we want to emphasize is the difference among the laws (2), (3), and (5). All the three laws have the function of stabilizing unstable orbits and same level of robustness to external noise [8]. However, the law (3) and (5) have the tracking function which is able to follow the desired orbit when system parameters vary slowly (even the variation is internal and/or random) [8]. The reason is that the desired objective x_* is not included in the laws explicitly and the perturbations can force the system state trajectory to pursue the changed position of the desired orbit automatically. This tracking technique is different from that [4,5] based on the OGY method where one has to *guess* or *predict* the changed position in advance.

The difference between Eqs. (5) and (3) is that the validity of Eq. (5) is guaranteed as long as the system is control-

*Electronic address: zhaoh@lzu.edu.cn
†Mailing address.

lable while this may not true for Eq. (3). This is simply explained in the following. When the system parameter p is excited, the perturbed system becomes a two-dimensional system:

$$x_{i+1}=f(x_i,p_i), \tag{6}$$

$$p_{i+1}=g(x_i,p_i). \tag{7}$$

To stabilize the desired fixed point is to find a suitable function g which makes the amplitudes of the two eigenvalues of the Jacobian matrix T smaller than one. Mathematically, to guarantee the solutions of the problem in any case, the function g should be a function which can give any specific eigenvalues λ_1 and λ_2 when $\partial f/\partial x$ and $\partial f/\partial p$ are given. It is easy to show that the equations determining the suitable g for fixed λ_1 and λ_2 are

$$\frac{\partial f}{\partial x}\frac{\partial g}{\partial p}-\frac{\partial f}{\partial p}\frac{\partial g}{\partial x}=\lambda_1\lambda_2, \quad \frac{\partial f}{\partial x}+\frac{\partial g}{\partial p}=-(\lambda_1+\lambda_2).$$

Thus, at least two adjustable coefficients should be included into the function g in order to guarantee the solution in general cases. One can see that the law (5) can satisfy this requirement while Eq. (3) cannot.

In contrast to the control laws (2) and (3), the control law (5) has another appropriate function, i.e., to target the unstable orbit from the stable one created at the same tangential bifurcation point without knowing the position of the unstable one in advance. This function provides another possible way to devise a new type of switch using the behavior of the tangent bifurcation instead of the bistability. In a bistable system, generally, there are two stable branches (or states) and a middle unstable branch (or state). In experiment, one can only observe the two stable branches by varying the system parameters, and the middle branch can never be observed from the system output because it is unstable. How to get the unstable middle state is considered as a particularly interesting subject [10–12]. In this paper, we will show that the applications of the feedback law (5) can provide a more general and effective way for experimentally observing the unstable middle branch in a bistable device.

However, the original form [8] of the control law (5) has not drawn much attention of experimentalists. An important reason may be due to the complication in obtaining the suitable coefficients. In this paper, we will introduce a simplified form of the feedback law and suggest a convenient way of implementation in experiments: only using the information of the time series measured from the system output and obtaining the suitable coefficients by simple analyses. The validity of the simplified control law is guaranteed for weakly unstable systems (systems near bifurcation points are important examples of the weakly unstable ones). Moreover, the examples in this paper show that the validity region is sufficiently wide in general, at least wider than that of the feedback law (3).

In the next section we derive the simplified control law based on the rigid results of Ref. [9]. Section III gives numerical results of applying the law to various systems with underlying equations described by the Hénon map, a time-delayed differential equation, and a coupled map lattice, respectively. In the last section of this paper, the results are summarized and discussed.

II. SIMPLIFIED CONTROL LAW

In this section, we derive a simplified control law of the form (5) based on the theoretical analyses of Refs. [8,9]. When one perturbs an original n-dimensional system

$$\mathbf{x}_{i+1}=f(\mathbf{x}_i,p), \tag{8}$$

by adding control to the external parameter p as

$$p_{i+1}=g(\mathbf{x}_i,p_i),$$

the system becomes an $(n+1)$-dimensional system and its stability can be determined by the eigenvalues of the Jacobian matrix

$$T=\begin{bmatrix} \frac{\partial f}{\partial \mathbf{x}} & \frac{\partial f}{\partial p} \\ \frac{\partial g}{\partial \mathbf{x}} & \frac{\partial g}{\partial p} \end{bmatrix},$$

where $\partial g/\partial \mathbf{x}$ and $\partial g/\partial p$ need to be determined. For nonsingular $\partial f \partial \mathbf{x}$ and $\partial f \partial p$, to make T always stable it demands [9] a suitable control function g with $(n+1)$ adjustable coefficients. [The only exception is the prompt linear feedback of type (2) where only n coefficients can guarantee the existence of the solution.] Thus, when adopting a control law of the type (5), one needs to construct the law as

$$p_{i+1}=p_0+\mathbf{k}(\mathbf{x}_{i+1}-\mathbf{x}_i)+k'(p_i-p_0), \tag{9}$$

where $\mathbf{k}\in\mathbb{R}^{\mathbf{n}}$. To simplify Eq. (9), we need to introduce the concept of stability region. The stability region is defined as the region in the coefficient space $(\mathbf{k},k')$, in which any point in it can make all the eigenvalues of the matrix T have amplitudes smaller than one. Following the procedure of Ref. [9], we can show that the stability region always exists for a fixed point $\mathbf{x}_*$ with nonsingular $\partial f/\partial \mathbf{x}$ and $\partial f/\partial p$. Since the calculation only needs the data of $\partial f/\partial \mathbf{x}$ and $\partial f/\partial p$ which can be obtained in principle from an experimental time series using the well-known delay coordinate embedding technique, the control law (9) can be used in experimental systems without knowing their underlying mathematical models, just like the prompt linear feedback law. However, to measure the derivative behaviors ($\partial f/\partial \mathbf{x}$ and $\partial f/\partial p$), a high-quality time series is required, otherwise the deviation of the solutions will be too big to make the calculation valid. Usually, a high-quality time series is not available in practice, especially when the underlying dynamics is high dimensional.

The stability region changes continuously with the eigenvalues of $\partial f/\partial \mathbf{x}$. In the case that $\mathbf{x}_*$ is initially stable, the stability region should be a region in the coefficient space around the origin $(\mathbf{k},k')$. When the fixed point becomes unstable, i.e., when the maximal amplitude of eigenvalues of $\partial f/\partial \mathbf{x}$ alters from a value smaller than 1 to a value greater than 1, the stability region will depart from the original continuously. As long as the amplitude of the maximal eigen-

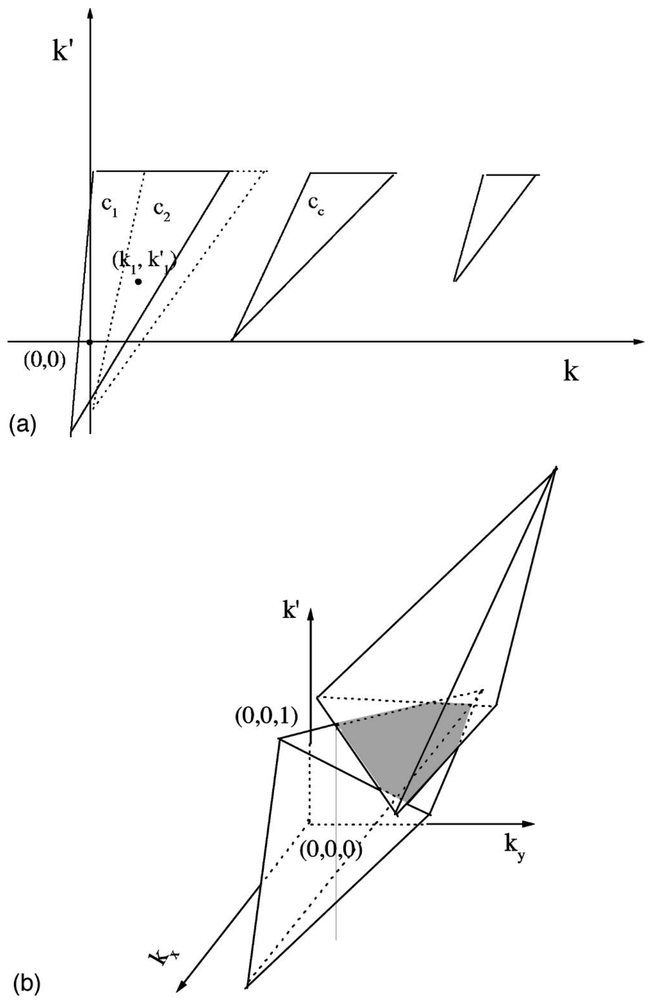

FIG. 1. (a) The evolution of the stability cross section in the k-k' plane. (b) Schematic stability regions of the stable (down-tetrahedron) and the unstable (up-tetrahedron) periodic orbits in the vicinity of a tangential bifurcation point for a two-dimensional map. The two tetrahedrons are separated exactly by the hyperplane $k'=1$.

value remains relatively small, one can reasonably expect that the stability region should lie in the vicinity of the origin.

Now, let us consider a plane k-k' passing through the origin of the coefficient space. In the case that the fixed point is initially stable, the plane must intersect with the stability region. When the amplitude of the maximal eigenvalue of $\mathbf{x}_*$ varies from a value smaller than one to a value greater than 1 and becomes bigger and bigger, one can easily imagine that the cross section should evolve as schematically shown in Fig. 1(a). The cross-section may disappear totally when the amplitude becomes big enough, i.e., the desired orbit becomes strongly unstable. This feature stirs our motivation to simplify the control law (9). Without lose of generality, we can take the measured signal of an experimental system as the first components x_i of the system state vector $\mathbf{x_i}=(x_i, x_{i-d}, x_{i-2d}, \ldots)$ from the view point of delay coordinate embedding technique. Notice that the parameter p_i is also available from the history records. Thus, we can apply x_i and p_i to construct a control law:

$$p_{i+1}=p_0+k(x_{i+1}-x_i)+k'(p_i-p_0). \qquad (10)$$

In the case that the desired fixed point is weakly unstable, the plane k-k' should have a cross section with the stability region and therefore the fixed point can be stabilized using the control law (10). In this way one avoids the application of the delayed coordinate embedding technique which demands a measurement of the derivative qualities $\partial f/\partial \mathbf{x}$ and $\partial f/\partial p$. As mentioned above, the use of the delay coordinate embedding technique asks for high quality time series which is indeed very difficult to get for a lot of real-world systems. Therefore, we expect that the simplified law should extend the scope of experimental applications of dynamical control.

Fixing $k'=0$ in Eq. (10), the law reduces to the Pyragas' control law. So the Pyragas' control law is not only a simplified form of Eq. (9) but also a simplified one of Eq. (10). Though all these laws can be used to stabilize and track the unstable fixed point without knowing its position in advance, we suggest to use the latter instead of the former for the following reasons. If the underlying dynamics of the experimental system is one dimensional, the control law (10) can always guarantee the validity of the control while the Pyragas' law cannot, as pointed out in the introduction section. In the case that the system is governed by an n-dimensional model, the simplified law remains effective if there exists the cross section between the subspaces [i.e., the axis k in the case of Pyragas' control law and the plane k-k' in the case of Eq. (10)] and the $(n+1)$-dimensional stability region. In general, the cross section for the plane k-k' can exist in a wider parameter region than that of the axis k. This statement can be easily understood from the demonstration of Fig. 1(a): the interval of the cross section on k axis (i.e., the Pyragas' case) vanishes at c_c after which the down-triangle [the case of law (10)] remains to exist in a certain parameter region.

The coefficients k and k' can be obtained by scanning the coefficient plane, as done by Pyragas to find the coefficient k in his control law. In addition, one can also catch them by the following tracking procedure. Let c_1 and c_2 be two close values of bifurcation parameter, where c_1 is smaller and c_2 is larger than the bifurcation point. According to the above analyses, the cross sections of c_1 and c_2 should exist, and they must overlap as long as c_1 and c_2 is close enough, as shown in Fig. 1(a). When we choose a point in the overlap region and adjust the parameter from c_1 to c_2 slowly, the system trajectory will be forced to track the fixed point automatically. Technically, it is easy to find points in the overlap region by simply trying several times. At c_1, we pick up a point, say (k_1, k_1'), close to the origin and apply it to the system following the law (10). If the fixed point remains stable constantly when adjusting the parameter from c_1 to c_2, then we catch the right coefficients, and at the mean time we get the idea in which direction we shall find the next point of coefficients when further adjusting the system parameter, i.e., if $k_1>0$ we can imagine that the cross section should move to the right when further increasing c, otherwise $k_1<0$ indicate an opposite result.

The prerequisite of applying this procedure is that the desired fixed point must still exist after the bifurcation as the cases of Hopf bifurcation and period-doubling bifurcations. In the case of tangent bifurcation, a pair of the fixed points appear simultaneously, with one stable and the other unstable. So one cannot apply the above procedure to the tangent bifurcation since no fixed point exist at all in one side of the bifurcation point. In this situation if one needs the system to work on the unstable fixed point instead of the stable one, what can one do? One must find a control law to force the system trajectory to leave the stable one and evolve to the unstable one. Generally, one may not know the position of the unstable fixed point in advance. The answer to this problem is to use the control law (9) or more conveniently to apply the law (10) again. In order to explain how to apply the law in this situation, we need to know more detailed knowledge about the stability regions of the pair of fixed points created from a tangent bifurcation. We have shown [9] that the stability regions of the stable orbit $\mathbf{x}_1$ and the unstable one $\mathbf{x}_2$ are separated by a hyperplane $k'=1$, and the former is below the hyperplane while the latter above, as show schematically in Fig. 1(b). Furthermore, the bottoms of the two stability regions on the hyperplane are partly overlapped [the shadow region in Fig. 1(b)]. Let $(k_1,k_2,\ldots,k_n,1)$ be a point on the shadow region. It is easy to see that the point $(k_1,k_2,\ldots,k_n,1-\delta)$ must be located in the stability regions of $\mathbf{x}_1$ and the point $(k_1,k_2,\ldots,k_n,1+\delta)$ in that of $\mathbf{x}_2$, where δ is a small positive number. This feature indicates that one can control the stability of $\mathbf{x}_1$ and $\mathbf{x}_2$ by applying the law (9) with the points of $1-\delta$ and $1+\delta$, respectively. When the system is close to the bifurcation point enough, the subspace k_1-k' should intersect with the shadow region, which implies that the point $(k_1,0,\ldots,0,1-\delta)$ and the point $(k_1,0,\ldots,0,1+\delta)$ are located within the inner of the stability regions of $\mathbf{x}_1$ and $\mathbf{x}_2$, respectively. In the other words, when we perturb the system according to the feedback law (10) with $(k,k')=(k_1,1-\delta)$ then $\mathbf{x}_1$ is stable and $\mathbf{x}_2$ remains unstable, but when one perturbs the system with $(k,k')=(k_1,1+\delta)$ then $\mathbf{x}_1$ becomes unstable and at the mean time $\mathbf{x}_2$ becomes stable, therefore the system trajectory will depart from $\mathbf{x}_1$ and evolve towards $\mathbf{x}_2$ automatically. Thus for the purpose of targeting $\mathbf{x}_2$ from $\mathbf{x}_1$, the feedback law (9) can be replaced by Eq. (10). The suitable value of k, although it is different from a system to another, can be easily found in experiments since we know that it must be close to zero (since the system is close the bifurcation point). Once one obtains a suitable value of k, one can switch the motion of the system between the two fixed points by adding perturbations with $(k,1\pm\delta)$ alternatively.

The above analyses confirm the validity of the law (10) when the system is close enough to a bifurcation point. How far it remains effective must be different for different systems. The following examples examine the validity of the law for systems with underlying mathematical models described by a finite-dimensional map, a time-delayed differential equation and a coupled map lattice, respectively. We will see that the parameter region in which the law (10) remains effective is very wide, usually far into the chaotic parameter region.

III. NUMERICAL EXAMPLES

As the first example we consider the case of the Hénon map $(x',y')=(1-ax^2+by,x)$, where a is assumed to be the bifurcation parameter and b the parameter which can be perturbed around $b_0=0.3$ within $\delta b=0.02$. In order to show the success of the feedback law (10) for high-periodic orbits, we pick up a period-7 orbit created at $a=1.2267$ through a tangent bifurcation. This orbit loses its stability through a period-doubling bifurcation at $a=1.254$. Adding feedback $b_{i+1}=b_0+k(x_{i+1}-x_i)+k'(b_i-b_0)$ to the system (x_i and b_i are recorded in every seventh iterations) with $k'=0$, we find that the periodic orbit can be tracked to $a=1.274$ from $a=1.25$ by suitably adjusting k from -0.1 to -1. Then fixing k' to 0.5 and adjusting k suitably we find that it can further be tracked to $a=1.30$. Clearly, the parameter region where the desired unstable orbit can be tracked by using the law (10) is wider than that of Pyragas' law.

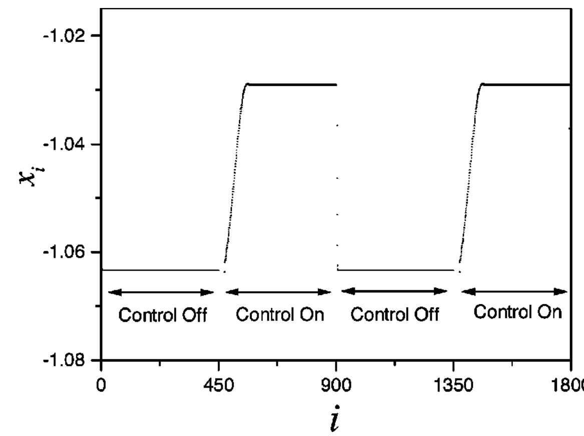

FIG. 2. Switching the dynamics between the stable and unstable period-7 orbits created by a tangent bifurcation using the control law (10).

To simulate the experimental systems, let us assume that we do not know the position of the unstable period-7 orbit in advance. At $a=1.23$ the system trajectory settles down on the stable period-7 orbit without controlling. We implement feedbacks to the system according to the law (10) with $k=-0.65$ and $k'=1.02$. Figure 2 shows that the trajectory is driven towards the stable orbit. When we cancel the control after the state trajectory settles down on the unstable orbit, the trajectory returns to the stable one again. Repeating the above procedure, we can switch the system output between the stable and the unstable orbits alternately, as shown in Fig. 2.

Our second example is a system described by $\tau\dot{x}(t)=-x(t)+\mu\sin^2[x(t-1)-x_B]$, which is a time-delayed differential equation with an infinite number of degrees of freedom and is applied as a model of laser device constantly [13]. In this equation the evolution time t is measured in the unit of the delay time. The most interesting behavior of the system is the bistability. In Fig. 3(a) we fix $\tau=0.4$ and $x_B=3.0$ and plot x_i against μ, where $x_i=x(i)$ [i.e., the value of $x(t)$ measured at $t=i$]. In this figure the S-shaped bistable solution curve is the stationary solution of the system. The upper and lower branches of the curve are stable and the middle branch is unstable. With the increase of μ the upper branch loses its stability at $\mu=2.06$ through a Hopf bifurcation, and at the mean time a stable limit cycle appears. When μ increases further, the limit cycle loses its stability at $\mu=2.53$ and then a stable period-doubling limit cycle appears.

We first show the results of tracking the stationary solution corresponding to the upper branch of the S-shaped curve and the limit cycle created by a Hopf bifurcation, respectively. Here we take μ as our feedback parameter, i.e., we

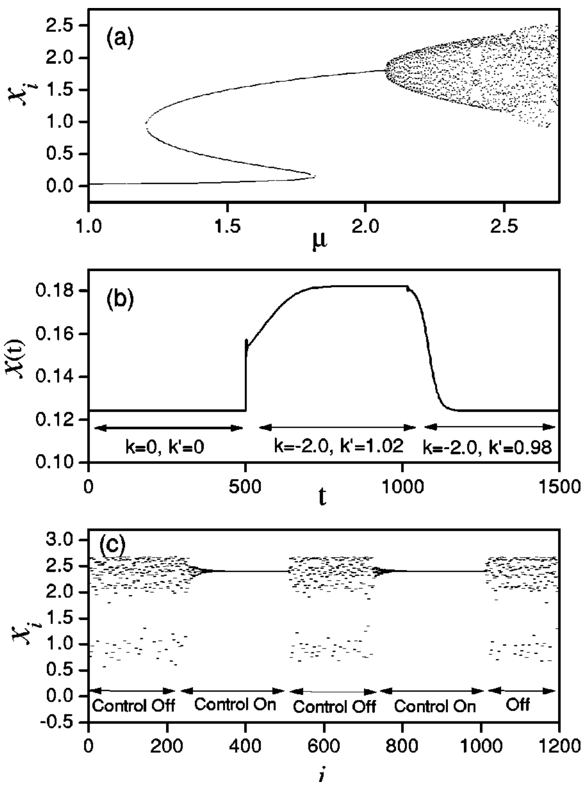

FIG. 3. (a) The bifurcation diagram of x_i versus μ, where $x_i = x(i)$. The upper branch and the lower branch are the stationary solutions of the system while the middle branch is the unstable stationary solution. The upper branch bifurcates into a limit cycle through a Hopf bifurcation at $\mu = 2.06$ and the limit cycle itself bifurcates into a period-doubling limit cycle at $\mu = 2.53$. (b) Switching the motion between the lower and the middle branches and (c) between the unstable limit cycle and the chaotic motion by using the feedback law (10).

add feedbacks $\mu_{i+1} = \mu_0 + k(x_{i+1} - x_i) + k'(\mu_i - \mu_0)$. In the case of stationary solution, the objective to be tracked appears as a fixed point in the discrete version. We can put $x_i = x(i)$ to the feedback law. It is found that the desired objective can be tracked only to $\mu = 2.08$ from $\mu = 2.05$ when we fix $k' = 0$ and adjust k suitably. Then fixing $k' = 0.5$ and adjusting k suitably, we can track it to $\mu = 2.22$ at least. In the case of the limit cycle, the time series of x_i measured in the above way generally appears as a quasiperiodic orbit since the period of the limit cycle is generally not a rational number. In this case we need a different way to measure x_i. We record $x(t)$ at time $t_i - \delta$ as x_i, i.e., $x_i = x(t_i - \delta)$, where t_i denotes the time at the ith $x(t)$ crossing the surface of section $x(t) = 1.8$ and δ is a positive number limited in the interval $0 < \delta < 1$. In this way one may get an infinite number of different time series with different values of δ, which corresponds to the feature of the infinite degrees of the delay systems. In the neighborhood of the bifurcation point, numerical calculations indicate that the tracking procedure may be effective by using $x_i(t_i - \delta)$ with an arbitrary δ. In general, the parameter region in which the feedback law keeps valid depends closely on the coefficient k' too. For example, in the case of $\delta = 0.8$, when we fix $k' = 0$ and adjust k suitably, the limit cycle can be tracked to $\mu = 2.75$ from $\mu = 2.53$. When fixing $k' = 0.5$ and adjusting k, we find that it can further be tracked to $\mu = 3.0$, which is already located in the chaotic region. Fig. 3(c) shows the result of switching the motion of the system between the limit cycle and the chaotic motion at $\mu = 2.95$, where $k = 0.8$ and $k' = 0.5$ in the ''control on'' sections.

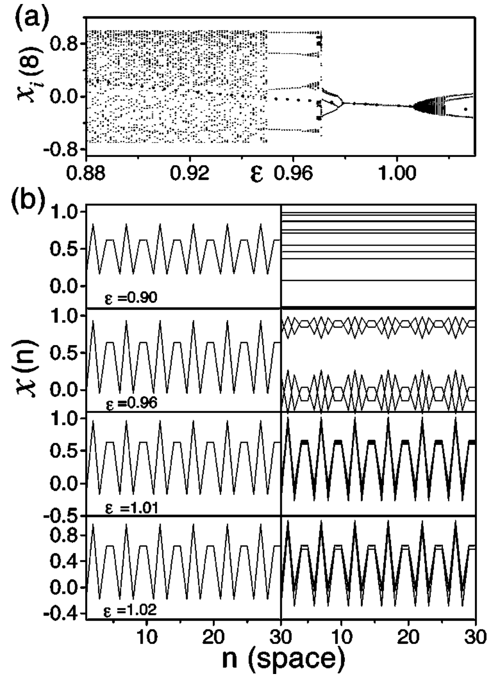

FIG. 4. (a) Bifurcation process of a pattern of the coupled logistic lattice. (b) The tracked patterns (first column) and the corresponding uncontroled patterns (second column). For clearification only 30 lattices are shown.

Next, we discuss the problem of targeting the middle branch of the *S*-shaped curve from the upper or lower branches. This problem can also be expressed as switching the dynamical motion of the system between the branches of the *S*-shaped curve. In fact, the two turning points of the *S*-shaped curve are tangential bifurcation points. Therefore it is just the place to use the targeting function of the control law (10). Let us consider the lower and the middle branches as an example. From Fig. 3(a) we find that $\mu = 1.82$ is the turning point of the lower and the middle branches. According to Eq. (10) we add perturbations to the parameter μ with $k = -2.0$ and $k' = 1.02$ at $\mu = 1.80$, where $x_i = x(i)$. Figure 3(b) shows that the system trajectory initially lying in the lower branch is driven to the middle branch. After the system trajectory settles down on the middle branch, one can add feedbacks with $k = -2.0$ and $k' = 0.98$ to perturb it to return to the lower branch. In this way we can switch the motion between the two branches at will, as shown in Fig. 3(b).

When the system trajectory settles down on the middle branch, the tracking function of the law can be applied to obtain the whole middle branch, see Fig. 3(a). The tracking procedure may fail when the parameters are far from the bifurcation point, which occurs generally for high-dimensional systems, then one has to use the feedback law (9) instead of (10).

The last example is a spatiotemporal system described by the coupled logistic lattice, $x_{i+1}(n) = (1-\varepsilon) f(x_i(n)) + 0.5\varepsilon[f(x_i(n-1)) + f(x_i(n+1))] + c$, where i is the discrete time, n the lattice site, ε the lattice coupling constant, and $f(x)=1-ax^2$. c is a parameter that we add to the system to imitate an external adjustable constant field which can be adjusted around $c=0$. Periodic boundary conditions are used throughout. Our controlling objective is a pattern found at $a=1.7$ and $\varepsilon=0.99$ with $N=60$. This is a period-1 solution of the system. Figure 4(a) shows the bifurcation process of the pattern represented by $x_i(8)$ against ε at $a=1.7$. In the direction of decreasing ε, the desired pattern loses its stability through a period-doubling bifurcation at $\varepsilon=0.98$. Adding feedbacks $c_{i+1}=k[x_{i+1}(8)-x_i(8)]+k'(c_i-c_0)$ to the system at $\varepsilon=0.98$ and adjusting k in a interval (0.1,0.35) suitably with $k'=0$, we can track the pattern to $\varepsilon=0.864$, where the desired pattern contracts to a line $x_*(1)=x_*(2)=x_*(3)=\cdots=x_*(60)=0.5273$.

On the other hand, the desired pattern loses its stability through a Hopf bifurcation with the increase of ε at $\varepsilon=1.006$. We add feedbacks to the system and adjust k in the interval $(-0.01,-0.24)$ with $k'=0$, the pattern is tracked to $\varepsilon=1.02$. Again, when we adjust k and k' simultaneously it can be tracked at least to $\varepsilon=1.05$. In the first column of Fig. 4(b), we show the tracked patterns at the corresponding parameters designated in the figure. When we cancel the control, these patterns will be replaced by new patterns immediately, see the second column of Fig. 4(b). In general, time series measured at any lattice can be used to realize the above purpose with a slightly difference of control ability. However, exceptions can also be found. For some patterns, there exists the case that the time series measured at a lattice shows bifurcation while the output from another lattice exhibits no impression of the phenomenon. In this case the control based on the output of the latter lattice would be invalid.

IV. CONCLUSIONS

In this paper, we introduced a simple but general feedback law for the purpose of controlling the dynamical behaviors in the neighborhood of the bifurcation point with experimental signals. The feedback law retains all the functions of the feedback law (9), i.e., stabilizing, tracking, and targeting the unstable orbits, but the requirement of the quality of the experimental time series is soften dramatically since it does not need to use a delay coordinate embedding technique to calculate the feedback coefficients. Even though the validity of the simplified law is guaranteed for weakly unstable systems in principle, our numerical calculations have shown that it is usually sufficiently useful for practical applications even in spatiotemporal systems.

We would like to point out that the well-known Pyragas' control law is a special form of the control law introduced in this paper, i.e., a special case of $k'=0$. We have especially emphasized that the latter law is more powerful than the former in our numerical examples by comparing the parameter regime in which the law is effective.

ACKNOWLEDGMENTS

We acknowledge fruitful discussions with Dr. Changsong Zhou. This work was supported in part by the National Basic Research Project ''Nonlinear Science,'' the National Natural Science Foundation of China and the Doctoral Education Foundation of China.

[1] F.J. Romeiras, C. Grebogi, E. Ott, and W.P. Dayawansa, Physica D **58**, 165 (1992).
[2] E. Ott, C. Grebogi, and A. Yorke, Phys. Rev. Lett. **64**, 1196 (1990); Phys. Rev. E **64**, 2837 (1990).
[3] A. Garfinkel, M.L. Spano, W.L. Ditto, and J.N. Weiss, Science **257**, 1230 (1992).
[4] Z. Gills, C. Iwata, R. Roy, I. Schwartz, and I. Triandaf, Phys. Rev. Lett. **69**, 3169 (1992); T. Carroll, I. Triandaf, I. Schwartz, and L. Pecora, Phys. Rev. A **46**, 6189 (1992).
[5] I. Triandaf and I. Schwartz, Phys. Rev. E **48**, 718 (1993); Phys. Rev. A **46**, 7439 (1992).
[6] K. Pyragas, Phys. Lett. A **170**, 421 (1992); **181**, 203 (1993).
[7] A. Kittel, J. Parisi, and K. Pyragas, Phys. Lett. A **198**, 433 (1995); K. Pyragas and A. Tamasevicius, *ibid.* **180**, 99 (1993); A. Kittel, J. Parisi, K. Pyragas, and R. Richter, Z. Naturforsch. A **49**, 843 (1994); S. Bielawski, M. Bouazaoui, D. Derozier, and P. Glorieux, Phys. Rev. A **47**, 3276 (1993).
[8] H. Zhao, J. Yan, J. Wang, and Y.H. Wang, Phys. Rev. E **53**, 299 (1996).
[9] H. Zhao, Y.H. Wang, and Z.B. Zhang, Phys. Rev. E **57**, 5358 (1998).
[10] E.C. Zimmermann, M. Schel, and J. Ross, J. Chem. Phys. **81**, 1327 (1984).
[11] B. Macke, J. Zemmouri, and N.E. Fettouhi, Phys. Rev. A **47**, R1609 (1993).
[12] G. Hu and K.F. He, Phys. Rev. Lett. **71**, 3794 (1993).
[13] J.P. Goedgebuer, L. Larger, and H. Porte, Phys. Rev. E **57**, 2795 (1998).